Original Article

DOI: 10.5582/bst.2024.01149

SEC24C suppresses the propagation and chemoresistance of hepatocellular carcinoma by promoting unfolded protein response-related apoptosis

Xuewen Tao[1,2,§], Haowei Wei[3,§], Shuai Mao[2,4,§], Jincheng Wang[2,5,§,*], Cailin Xue[3], Weiwei Yu[3], Yuze Shi[3], Yang Liu[1,2,*], Beicheng Sun[1,2,*]

[1] School of Medicine, Southeast University, Nanjing, Jiangsu, China;
[2] Department of General Surgery, The First Affiliated Hospital of Anhui Medical University, Hefei, Anhui, China;
[3] The Affiliated Drum Tower Hospital of Nanjing University Medical School, Nanjing, Jiangsu, China;
[4] Lianyungang oriental hospital, Lianyungang, Jiangsu, China;
[5] Graduate School of Medical Science and Engineering, Hokkaido University, Sapporo, Japan.

SUMMARY Cells routinely utilize the unfolded protein response (UPR) to alleviate endoplasmic reticulum (ER)-stress or trigger about apoptotic death under extreme ER-stress conditions. Tumor cells are subjected to persistent ER-stress due to their crowded microenvironment, but can maintain hyperactive proliferation under most stressful conditions. Therefore, understanding strategies employed by cancer cells to escape from UPR-related apoptosis has important medical implications. SEC24 homolog C (SEC24C) was found decreased in later colorectal cancer (CRC) stages, but its exact role in response to ER-stress and activation of UPR in hepatocellular carcinoma (HCC) remains to be elucidated. Here, we have identified the downregulation of SEC24C in human HCC sample and its suppressive role in regulating HCC proliferation and chemoresistance. Mechanistically, SEC24C was found to interact with eukaryotic translation initiation factor 2 alpha kinase 3 (EIF2AK3 or PERK) and activate the downstream UPR-related apoptosis. During this process, SEC24C was observed to be anchored in nucleus under normal condition but responded immediately to ER-stress and could subsequently translocate to the ER. Furthermore, overexpression of SEC24C significantly augmented the efficacy of bortezomib in HCC treatment. In conclusion, our findings revealed a novel role of SEC24C in regulating HCC proliferation and chemoresistance by modulating UPR activation.

Keywords hepatocellular carcinoma (HCC), unfolded protein response, chemotherapy

1. Introduction

Hepatocellular carcinoma (HCC) remains one of the most common cancers worldwide (*1*). Although significant advancements have been made, effective systemic therapies for management of HCC are limited. Recently, targeting the unfolded protein response (UPR) and redirecting it towards apoptosis has emerged as a promising approach in cancer therapy (*2,3*). The proteostasis of the ER is exquisitely maintained, but it has been found that various factors can disrupt the processes of protein synthesis and provoke the state of ER-stress. The intrinsic factors related to hyperactive proliferation and external factors of hypoxia as well as nutrient deprivation can cause cancer cells to experience persistent ER-stress (*4*). It has been reported that to alleviate the ER stress condition, a series of signaling pathways called UPR are induced (*5*). The different branches of the UPR act synergistically or antagonistically to promote the cell survival or induce apoptosis if ER stress remains unmitigated (*6*). The selective lysosomal degradation of specific ER fragments, termed ER-phagy, could also relieve ER-stress (*7*). And SEC24C, a subunit of the coat protein complex II (COPII), was observed to exhibit a noncanonical function in participating ER-phagy (*8*). Activating transcription factor 4 (ATF4), an important component of the UPR, has also been reported to function in ER-phagy (*9*), so we hypothesized that SEC24C may participate in the regulation of UPR. Besides, the downregulated expression of SEC24C in later colorectal cancer stages was both validated with gene expression commons platform meta-analysis and IHC experiments (*10*). Overall, it is speculated that SEC24C could effectively respond to ER-stress and

affect UPR to impact HCC progression. In the present study, we have shown that SEC24C could promote UPR-related apoptosis by promoting the dissociation of Bip from PERK, thus suppressing the proliferation and chemoresistance of HCC cells.

2. Materials and Methods

2.1. Human samples

HCC samples (including tumor and adjacent nontumor samples) were collected from patients between August 2019 and September 2022 at Nanjing Drum Tower Hospital. Normal human liver samples were obtained from hepatic hemangioma patients with no evidence of chronic liver disease, diabetes, or hypertension. All patients provided written consent. All studies were approved by the Institutional Ethics Committee of Nanjing Drum Tower Hospital in compliance with the 1975 Declaration of Helsinki.

2.2. *In vivo* experiments

BABL/c male nude mice, 6 weeks of age, were purchased from the animal center of Nanjing University (Nanjing, Jiangsu, China), raised and permitted by the Nanjing University animal studies committee. In the subcutaneous transplantation model, mice were distributed at random to each group (n = 6 or 5) and implanted with Huh7 sgSEC24C, Huh7 sgNC, MHCC97H OE-SEC24C, or MHCC97H NC cells in the right groin. The mice were euthanized at 4 weeks after implantation and calculated the volume of the tumors. The equation (length × height × width) × 0.52 was used to calculate the tumor volume. For tumor drug resistance research, each group was given an intravenous injection of bortezomib (1 mg/kg body weight) or Sal003 (2.5 mg/kg body weight) once per week for 3 weeks.

For the primary liver cancer model, $Trp53^{flox/flox}$ mice were a kind gift from Southern Medical University. $Trp53^{flox/flox}$ mice were crossed with Alb-Cre mice to generate hepatocyte-specific Trp53 knockout ($Trp53^{\Delta hep}$) mice. The mixture used for hydrodynamic intravenous injection included a sterile 0.9% NaCl solution/plasmid mix containing 5 μg of pSB-U6-sgSEC24C-TBG-Cas9 or 5 μg of pSB-TBG-SEC24C-FLAG, 5 μg of pSB-EF1α-Myc and 2.5 μg of CMV-SB_{13} transposase plasmids. A total volume of mixture corresponding to 10% of body weight was injected *via* the tail vein in 7 s into 8-week-old male $Trp53^{\Delta hep}$ mice. After 6 weeks, mice were humanely sacrificed by CO_2 asphyxiation. The equation (length × $width^2$) × 0.52 was used to calculate the tumor volume. All animal experiments were approved by the Animal Core Facility of Nanjing Drum Tower Hospital and were performed in accordance with guidelines for the care and use of laboratory animals.

2.3. Statistical analysis

All data presented were based on at least 3 independent experiments both *in vivo* and *in vitro*. Student's *t* test was used for comparisons among two groups and One-way ANOVA was used for comparisons between more than two groups. Survival analysis was performed with the Kaplan–Meier method. Statistically significant differences were considered only if $P < 0.05$. SPSS 19.0 and Prism 8 were utilized for data analysis. Additional experimental procedures are described in the Supplementary Materials and Methods (*https://www.biosciencetrends.com/supplementaldata/207*).

3. Results

3.1. SEC24C, a member of COPII, is frequently downregulated in HCC

To confirm the potential function of SEC24C in HCC, the mRNA and protein levels of SEC24C in HCC and corresponding adjacent normal tissues were first measured. As depicted in Figure 1A, The Cancer Genome Atlas (TCGA) and Genotype-Tissue Expression (GTEx) database indicated that expression of SEC24C was downregulated in the tumor tissues compared to normal tissues, which was also validated with qRT-PCR experiment of HCC samples from our tissue bank. Next, we examined the protein level of SEC24C in HCC tissues using immunohistochemical (IHC) staining and found downregulated SEC24C protein levels in HCC tissues (Figure 1B). Notably, SEC24C was primarily concentrated in the nucleus in the peritumor tissues but the tumor tissues have an obvious deficiency of SEC24C expression in the nucleus. Thereafter, we employed western blotting (WB) in 10 paired samples from HCC patients and 10 normal liver samples to confirm the downregulated SEC24C expression in HCC (Figures. 1C, 1D). And the downregulation of SEC24C was also found in the liver cirrhosis tissues (Supporting Figure S1A, *https://www.biosciencetrends.com/supplementaldata/207*). To further identify its prognostic value in HCC, Kaplan–Meier Plotter was used, and the results displayed that low expression of SEC24C was significantly correlated with the poor progression-free survival (PFS) and relapse-free survival (RFS). However, analysis of overall survival (OS) only exhibited a significant correlation between low SEC24C expression and poor prognosis for the male patients infected with hepatitis virus but not for all the patients (Figure 1E). Taken together, these results suggest that SEC24C might play a critical role in the development of HCC and significantly correlate with the prognosis of HCC patients.

3.2 SEC24C attenuates malignant phenotypes of HCC cells *in vitro*

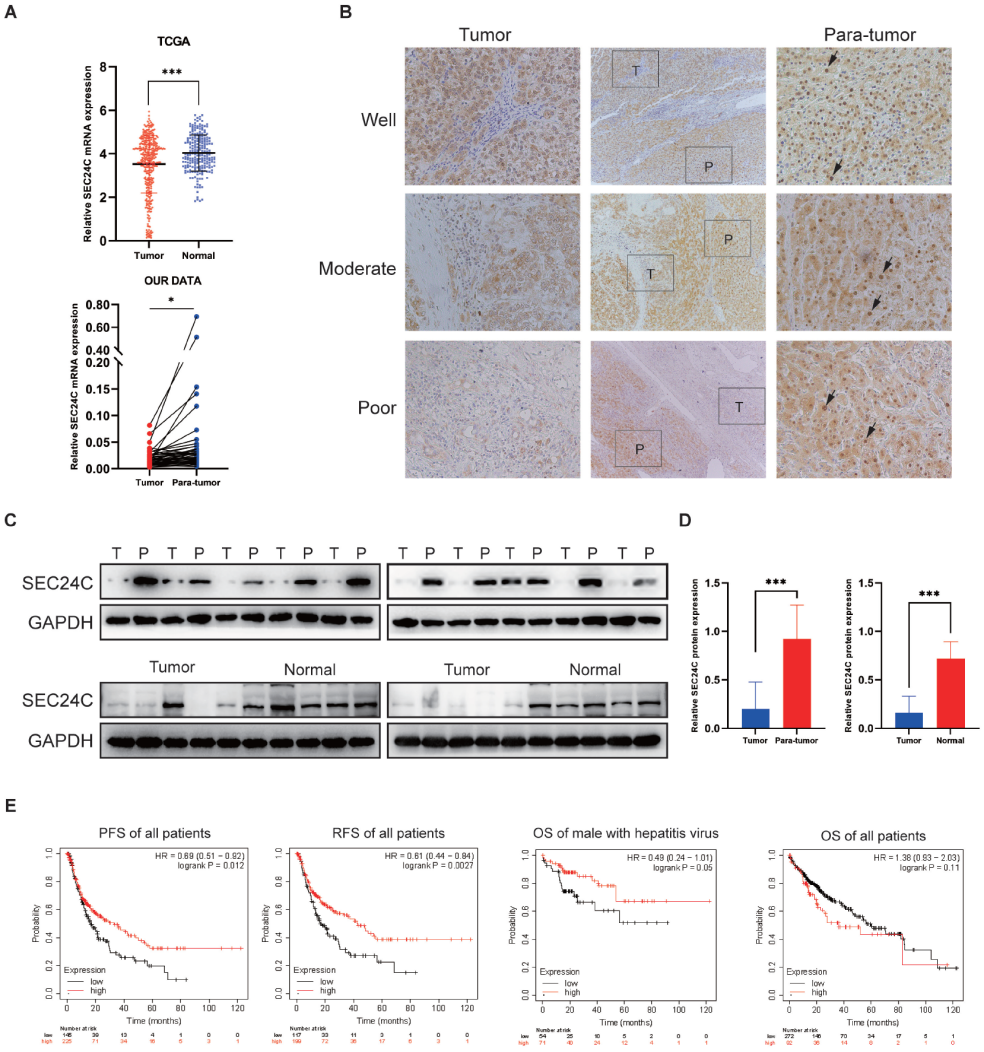

Figure 1. Downregulation of SEC24C in human HCC tissues. (A) The data regarding RNA expression of SEC24C for HCC patients obtained from the Cancer Genome Atlas, Genotype-Tissue Expression and our tissues bank were statistically analyzed (*$P < 0.05$; **$P < 0.01$; ***$P < 0.001$). **(B)** Representative IHC staining images of SEC24C in HCC tissues of different differentiation grades from HCC sections. Arrows: nuclear staining. **(C)** Representative expression levels of SEC24C protein in 10 paired HCC (T) and corresponding peritumor tissues (P), as well as 10 normal liver tissues, were analyzed by western blotting, and the quantification of SEC24C protein levels is depicted in **(D)** (**$P < 0.01$; ***$P < 0.001$). **(E)** Kaplan–Meier Plotter was used for the prognosis analysis in HCC patients stratified by high and low expression of SEC24C.

To confirm the antitumor activity of SEC24C in HCC, we first detected the protein levels of SEC24C in four different HCC cell lines as well as the immortalized hepatocytenormal liver cell line (HepaRG) by western blot analysis (Supporting Figure S1B, *https://www.biosciencetrends.com/supplementaldata/207*). Then, MHCC97H cells was selected to construct an *in vitro* overexpressing (OE) model as they showed relatively low expression of SEC24C. Similarly, Hep3B cells was chosen to establish SEC24C-silenced cell lines whereas SEC24C expression in the Huh7 cells was knocked out by CRISPR Cas9. WB verified SEC24C expression levels in the generated cell lines (Supporting Figure S1C, *https://www.biosciencetrends.com/supplementaldata/207*). Thereafter, plate colony formation and cell counting kit-8 (CCK8) assays showed that knockdown of SEC24C in Hep3B cells or knockout of SEC24C in Huh7 cells both significantly promoted the clone formation ability as well as proliferation rate. However, decreased colony formation and proliferation rates were observed in MHCC97H OE-SEC24C cells in comparison with control cells (Figure 2A-B). In addition, the effect of SEC24C on HCC migration and invasion was investigated *in vitro* (Figures 2C, 2D). Moreover, flow cytometry experiments were also performed and displayed that deletion of SEC24C in HCC cells significantly reduced the apoptotic rates (Figures 2E, 2F). These results indicated the suppressive role of SEC24C in regulating HCC cell proliferation and metastasis.

3.3. SEC24C weakens HCC progression *in vivo*

To further validate the impact of SEC24C on HCC, we performed tumorigenesis assays under *in vivo* conditions. A subcutaneous xenograft model was developed, and the results revealed that SEC24C overexpression

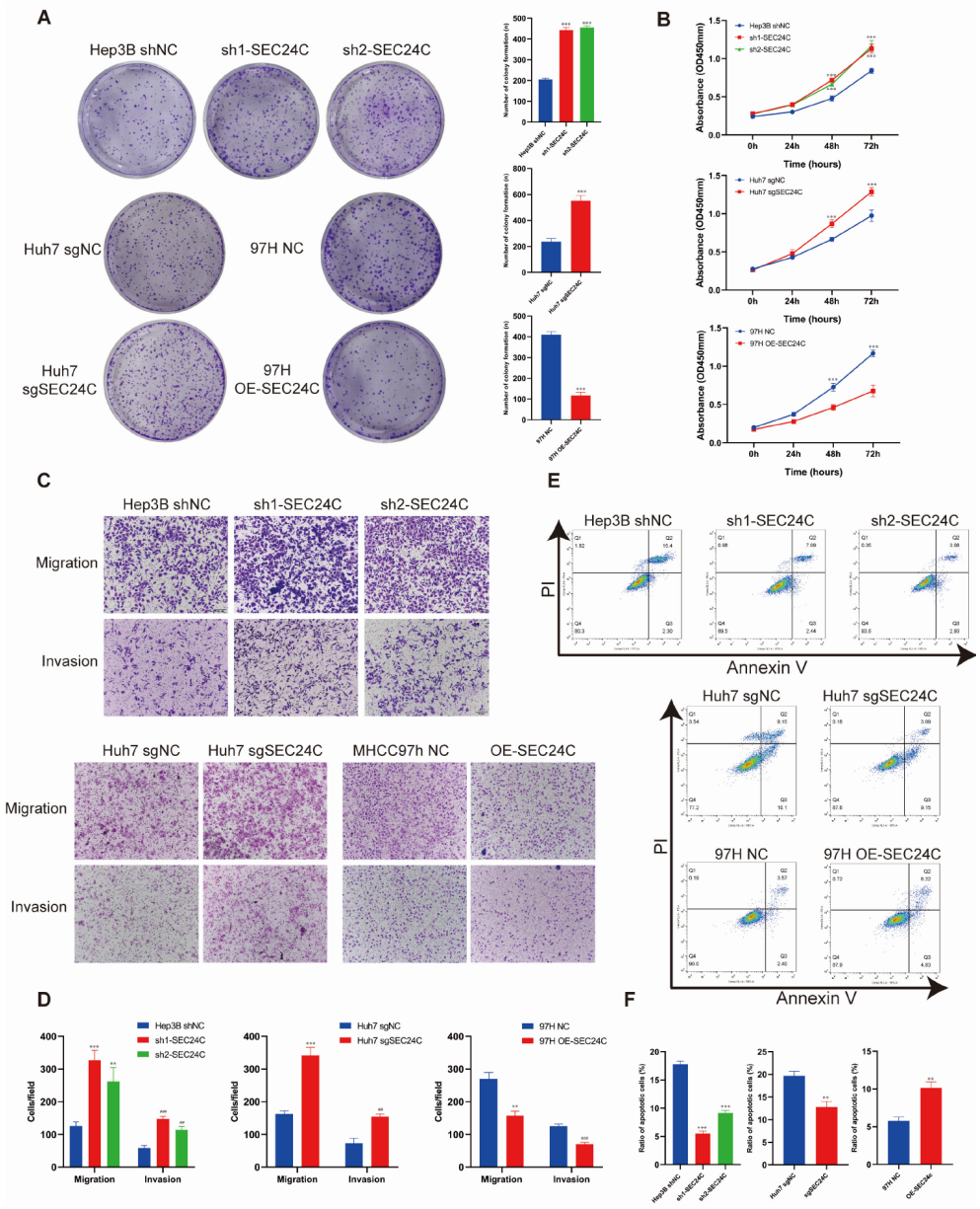

Figure 2. Tumor-suppressive functions of SEC24C in HCC cells. (A) Representative images of colony formation induced by Hep3B shNC, Hep3B sh1-SEC24C, Hep3B sh2-SEC24C, Huh7 sgNC, Huh7 sgSEC24C, MHCC97H NC and MHCC97H OE-SEC24C cells respectively. The numbers of colonies were counted and are shown in the right bar graph. **(B)** CCK8 assays of Hep3B sh1-SEC24C&sh2-SEC24C, Huh7 sgSEC24C, MHCC97H OE-SEC24C cells and the corresponding control cells. **(C)** Invasion and migration assays were performed in the presence or absence of matrix. The number of invaded and migrated cells was calculated and have been shown in bar graph **(D)**. **(E)** Apoptosis assays for Hep3B sh1-SEC24C&sh2-SEC24C, Huh7 sgSEC24C, MHCC97H OE-SEC24C cells and the corresponding control cells were performed after treatment with H_2O_2 using flow cytometry analysis. The apoptosis rate of the cells was measured and has been shown in the bar graph **(F)**. All experiments were performed in triplicate, and the data has been expressed as the mean ± SD from three independent experiments ($n = 3$, $^{**}P < 0.01$; $^{***}P < 0.001$; $^{\#\#}P < 0.01$; $^{\#\#\#}P < 0.001$)

significantly inhibited the tumor growth, whereas the SEC24C knockout promoted this process (Figure 3A). Furthermore, we created a primary liver cancer model (*11*) with liver-specific knockout or overexpression of SEC24C. We first generated the mice with hepatocyte-specific deletion of Trp53 ($Trp53^{\Delta hep}$) by crossing $Trp53^{flox/flox}$ mice with Alb-Cre mice, as 58% of HCC patients have been reported possess the Trp53 mutation (*12*). Thereafter, a CRISPR–Cas9 fraction of SEC24C (sgSEC24C-Cas9) and the SEC24C cDNA were cloned into the Sleeping Beauty (SB) vector respectively. These plasmids along with their control plasmids were then hydrodynamically injected in combination with pSB-EF1α-Myc and CMV-SB_{13} transposase plasmids through the tail vein in $Trp53^{\Delta hep}$ mice (Figures 3C, 3D). At 6 weeks after injection, the tumors from mice injected with SB-sgSEC24C-Cas9 plasmids exhibited a significantly increased number and volume in comparison with the controls. In contrast, tumors obtained from the mice injected with SB-SEC24C plasmids displayed a significant reduced number and volume in comparison with the controls (Figure 3E). Immunostaining with

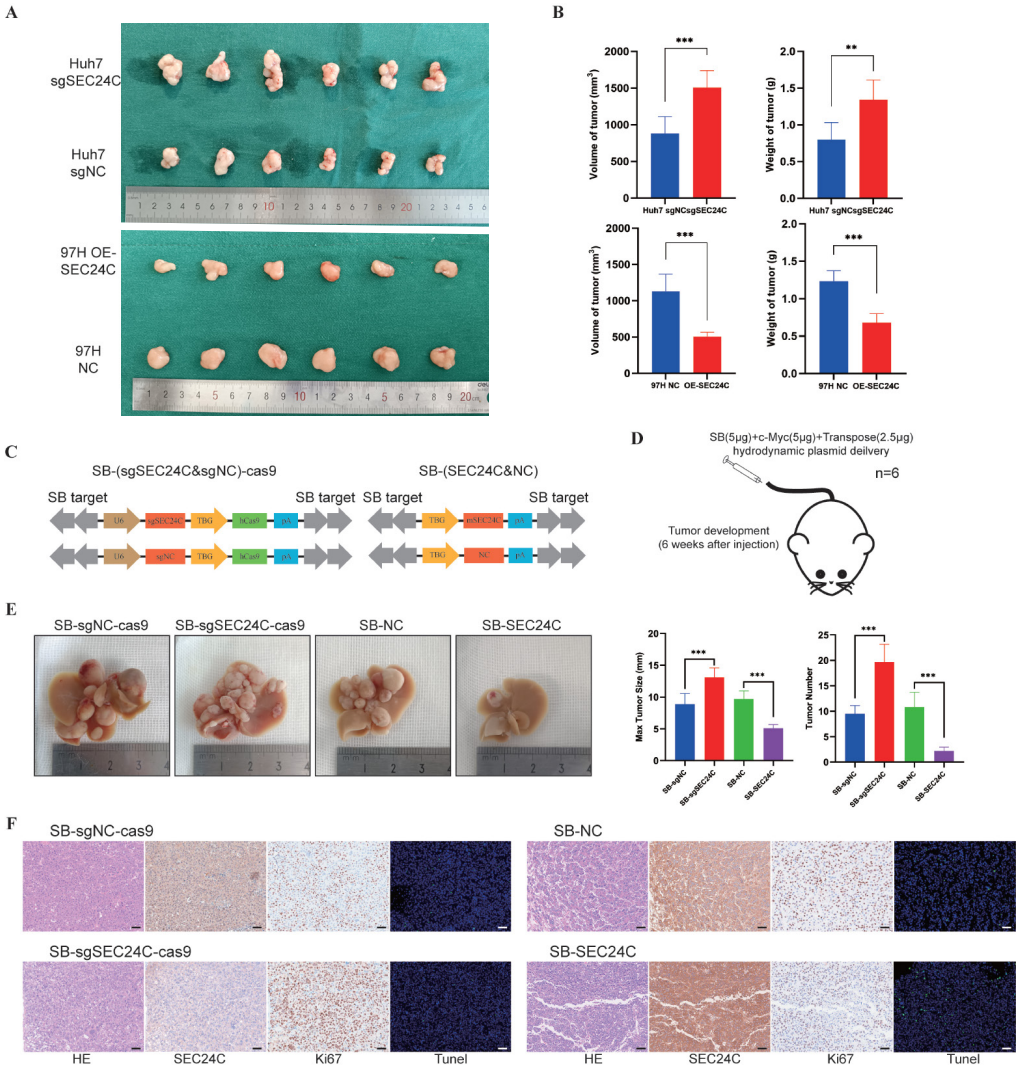

Figure 3. Tumor-suppressive effects of SEC24C *in vivo*. (A) Representative images have been shown for the tumors derived from the nude mice induced by Huh7 sgSEC24C and Huh7 sgNC cells (upper panel) and MHCC97H OE-SEC24C as well as MHCC97H NC cells (lower panel) after the subcutaneous injection. **(B)**The tumor volume and tumor weight were measured 30 days after implantation after sacrificing the mice ($n = 6$). **(C)** and **(D)** $Trp53^{\Delta hep}$ mice were utilized to establish a primary liver cancer model by hydrodynamic injection of SB-sgSEC24C-cas9 or SB-SEC24C and the corresponding control plasmids, as well as c-Myc and transpose plasmids. **(E)** Representative HCC samples of $Trp53^{\Delta hep}$ mice ($n = 6$) with the different plasmids. The number of the tumors was measured and has been shown in the right bar graph. **(F)** HE, SEC24C, ki67 and TUNEL staining were performed in HCC sections (scale bar: 50 μm). All results have been presented as the mean ± SD (**$P < 0.01$; ***$P < 0.001$).

Ki67 and TUNEL confirmed increased proliferation and alleviated apoptosis after specific knockout of SEC24C, whereas SEC24C overexpression led to an opposite outcome *in vivo* (Figure 3F). All these results suggested that depletion of SEC24C led to liver tumorigenesis as well as tumor progression.

3.4. SEC24C translocates from nucleus to ER upon ER-stress

In Figure 1B, we found that SEC24C was concentrated in the nucleus of peritumor tissues, but tumor tissues lacked the protein expression of SEC24C in nucleus. As SEC24C was mainly reported as a cytosolic protein to locate at the ER surface and could participate in ER-phagy (*8*), we deduced that SEC24C may be transferred from the nucleus to the ER surface under stressed conditions and then be degraded by autolysosome. Starvation and ER-stress both have been found to activate ER-phagy to restore ER homeostasis (*13,14*), so Earle's Balanced Salt Solution Earle's Balanced Salt Solution (EBSS) and tunicamycin (TM) are both employed to investigate whether SEC24C could be degraded during ER-phagy process. In support of our hypothesis, application of TM and EBSS resulted in a gradual upregulation of LC3 II protein levels and a reduction in receptor accessory protein 5 (REEP5), degradation of which was a marker for ER-phagy (*15*) (Figure 4A, and Supporting Figure S2A, *https://www.biosciencetrends.com/supplementaldata/207*). As the autophagy level was frequently active in multiple types of cancer, we further investigated whether ER-phagy was more hyperactive in HCC than in peritumor tissues by examining the protein levels of reticulon-3-long (RTN3L) (Figure 4B),

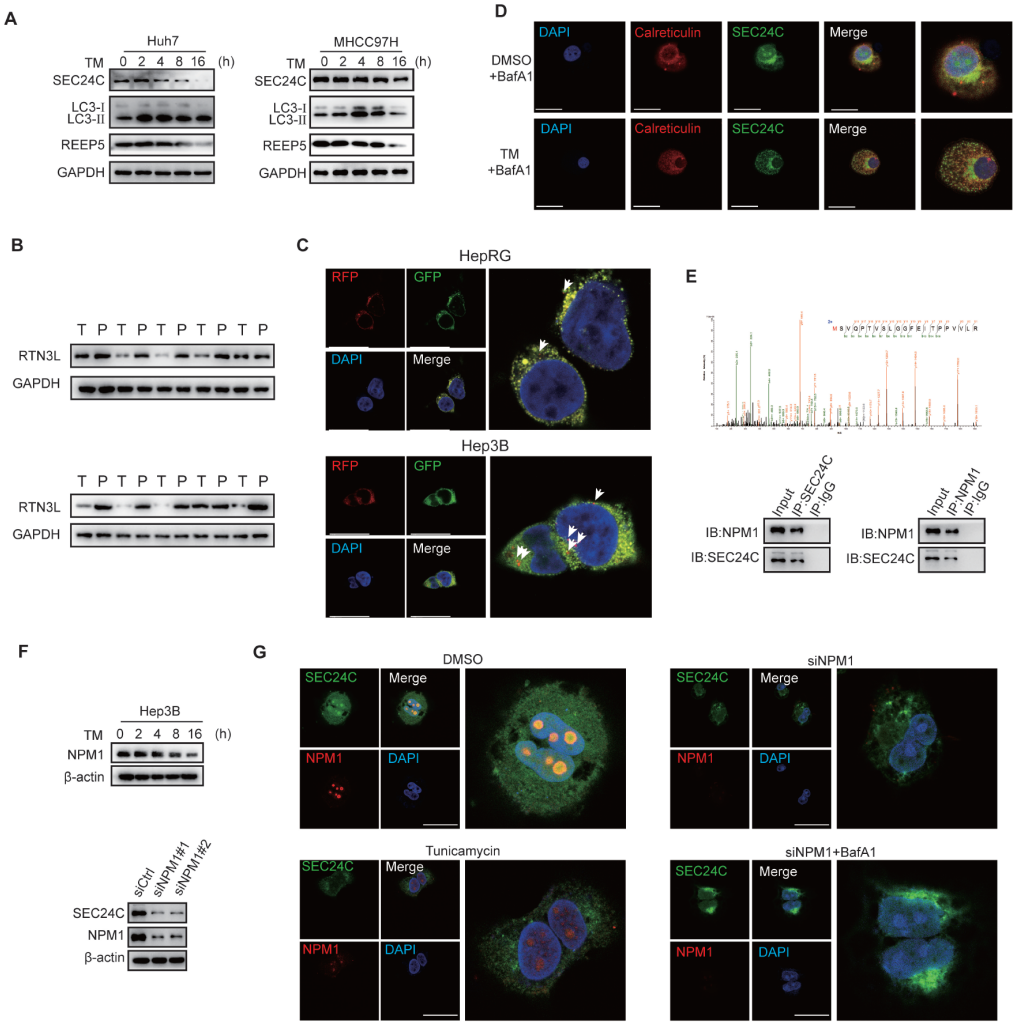

Figure 4. Degradation and shuttle of SEC24C under stress in HCC cells. (A) Representative images depicting the protein levels of SEC24C, LC3-I/II and REEP5 following TM treatment. **(B)** Representative expression levels of RTN3L protein in 10 paired HCC (T) and corresponding peritumor tissues (P) analyzed by western blotting. **(C)** Stable ssRFP-GFP-KDEL-expressing HepRG and Hep3B cells are under confocal microscopy of ssRFP$^+$/GFP$^-$KDEL$^-$ and ssRFP$^+$/GFP-KDEL$^+$ structures. Arrows highlight ssRFP$^+$/GFP-KDEL$^-$ puncta. **(D)** Representative images displaying the localization of SEC24C in Hep3B cells treated with DMSO or TM. **(E)** Collision-induced dissociation mass spectrum demonstrating the structural diagram of NPM1 protein (upper panel). SEC24C interacts with NPM1, as evidenced by a Co-IP assay in Hep3B cells (lower panel). **(F)** Representative images showing the protein levels of NPM1 upon TM treatment in Hep3B cells (upper panel) and SEC24C after NPM1 knockdown (lower panel). **(G)** Representative images depicting the localization of SEC24C and NPM1 with DMSO or TM (left panel). The concentration of SEC24C in the nucleus was attenuated by NPM1 knockdown and administration of BafA1 was able to restore the expression of SEC24C in the perinuclear area (right panel) in Hep3B cells (Scale bar: 50 μm). All experiments were performed in triplicate. Abbreviations: DAPI, 4′,6-diamidino-2-phenylindole; IgG, immunoglobulin.

which degradation are vital indicators of ER-phagy (*16*). Subsequently the ssRFP-GFP tandem fluorescently tagged KDEL plasmid was also employed to verify the specific ER-phagy process (*17*) and results revealed that Hep3B cell showed more numerous ssRFP$^+$/GFP-KDEL$^-$ puncta than HepRG cell (Figure 4C). Above data found that SEC24C are frequently degraded during ER-phagy and HCC has a hyperactive ER-phagy in most cases, suggesting that the decline of SEC24C in tumor tissue maybe partial due to persistent autolysosome degradation by ER-phagy in HCC.

Next, results of double immunofluorescent (IF) staining demonstrated that SEC24C could distribute in the nucleus and mainly localized within the nucleoli under normal condition, but upon TM treatment, SEC24C in the nucleus could effectively translocate at perinuclear ER surface (Figure 4D). In addition, cell fractionation analysis also confirmed the preferred localization of SEC24C in the nucleus under normal condition (Supporting Figure S2B, *https://www.biosciencetrends.com/supplementaldata/207*). To further unravel the shuttling mechanism of SEC24C, we performed liquid chromatography–tandem mass spectrometry (LC–MS/MS) and found that SEC24C interacted with nucleophosmin1 (NPM1) under normal condition, which could shuttle between cytoplasm and nucleus, and regulate protein nuclear translocation (*18-20*). Co-immunoprecipitation (Co-IP) experiments confirmed a direct interaction between SEC24C and NPM1 (Figure 4E). Then WB results found that NPM1

level was also decreased upon TM treatment (Figure 4F, upper panel). Thereafter, siRNAs targeted against NPM1 were used and an interesting fact was discovered that the SEC24C protein level decreased concomitantly with NPM1 reduction (Figure 4F, lower panel), but not the mRNA level of SEC24C (Supporting Figure S2C, *https://www.biosciencetrends.com/supplementaldata/207*). Use of bafilomycin A1 (BafA1) could restored the protein expression of SEC24C after NPM1 knockdown (Supporting Figure S2D, *https://www.biosciencetrends.com/supplementaldata/207*), implying that NPM1 may help SEC24C restore in the nucleus. Finally, IF analysis further verified that SEC24C was colocalized with NPM1 in the nucleus under normal condition. However, when ER-stress was induced, SEC24C dissociated from NPM1 and concentrated specifically in the perinuclear area (Figure 4G, left panel). After NPM1 knockdown, the distribution of SEC24C in nucleus was dismissed and application of BafA1 could rescue partial SEC24C expression in the perinuclear area (Figure 4G, right panel), which was also examined by cell fractionation analysis (Supporting Figure S2D, *https://www.biosciencetrends.com/supplementaldata/207*). To decrease possible interference from non-specific immunoreactivity of SEC24C antibody, SEC24C-Flag were constructed and transfected into Hep3B cells. Results of Co-IP and IF showed direct interaction of SEC24C and NPM1 in the nucleus by employing Flag antibody (Supporting Figures S2E, S2F, *https://www.biosciencetrends.com/supplementaldata/207*). Collectively, NPM1 could help SEC24C reserve in the nucleus under normal conditions, but upon ER-stress, SEC24C in the nucleus rapidly shuttled to the ER surface in HCC cells.

3.5. Loss of SEC24C facilitates HCC progression by suppressing the UPR

A number of studies have shown that the crowded molecular microenvironment can cause malignant cells particularly vulnerable to ER-stress (*4,21*) , and that activated UPR plays a critical role in HCC progression as well as survival (*22,23*). Our results have revealed the rapid response of SEC24C to ER-stress and demonstrated the shuttling of SEC24C from the nucleus to ER, thereby prompting us to speculate that SEC24C could participate in the process of ER-stress after localization in ER and thus suppress HCC proliferation by modulating the UPR. Interestingly, various past studies have revealed that SEC24C can effectively regulate specific cellular functions by interacting with the specific protein partners (*24,25*), hence we performed LC–MS/MS to qualitatively analyze the components of the SEC24C binding protein and identified a novel combination with both PERK (Figure 5A) and Bip (Supporting Figure S3A, *https://www.biosciencetrends.com/supplementaldata/207*). Co-IP experiments also showed a direct interaction between SEC24C and PERK (Figure 5B). However, considering that Bip is mainly localized in the ER lumen, but SEC24C lacks a transmembrane domain that can facilitate its access to the ER lumen, the association between SEC24C and Bip could be indirect and mediated by PERK.

Since the PERK branch remains the main studied signal for contributing to apoptotic death in UPR (*6,21,26*) and above results indicated that SEC24C had a strong impact on HCC apoptosis under both *in vitro* and *in vivo* settings (Figure 2F, 3F), we hypothesized that SEC24C could influence HCC cell apoptosis by modulating the PERK branch of UPR. WB results further verified that SEC24C knockout significantly decreased the protein levels of DNA damage inducible transcript 3 (DDIT3, also known as CHOP), a transcription factor downstream of PERK to promote apoptosis (*27*) (Figure 5C). Furthermore, immunoblotting data confirmed that SEC24C knockout significantly reduced the protein levels of phosphorylated PERK (p-PERK) in comparison to PERK and phosphorylated eukaryotic translation initiation factor 2 subunit alpha (eIF2α) (p-eIF2α) in comparison to eIF2α and ATF4, which was opposite in SEC24C-overexpressing group (Figure 5C), but was consistent in SEC24C knockdown cells (Supporting Figure S3B, *https://www.biosciencetrends.com/supplementaldata/207*). Moreover, results of qRT–PCR confirmed that the mRNA levels of CHOP and protein phosphatase 1 regulatory subunit 15A (PPP1R15A, also known as GADD34), which are transcriptional regulated downstream of UPR, were significantly positively correlated with SEC24C levels (Figure 5D). Interestingly, similar results were also obtained by WB analysis of HCC samples from $Trp53^{\Delta hep}$ mice injected with different SB plasmids (Figure 5E). And representative images of IHC staining showed that SEC24C knockout significantly reduced the protein expression and nuclear localization of p-PERK and CHOP, which was significantly enhanced upon SEC24C overexpression (Figure 5F).

To further analyze the function of SEC24C on PERK signaling, we examined the potential correlation between SEC24C and CHOP or GADD34 in TCGA database and observed significant positive correlations between SEC24C and all of them (Supporting Figure S3C, *https://www.biosciencetrends.com/supplementaldata/207*). In addition, we examined whether SEC24C affect UPR activation partly through its secretory role. As Sec24 isoforms have displayed overlapping selectivity for the different transport signals and some similarities in their secretory functions (*28*), we overexpressed the expression of three remain Sec24 isoforms in Huh7 sgSEC24C cells and knocked them down in MHCC97H OE-SEC24C cells. The results demonstrated no significant differences in the protein levels of CHOP after switching the three remaining Sec24 isoforms, thus suggesting that SEC24C can promote the activation of PERK signaling independent of its secretory function

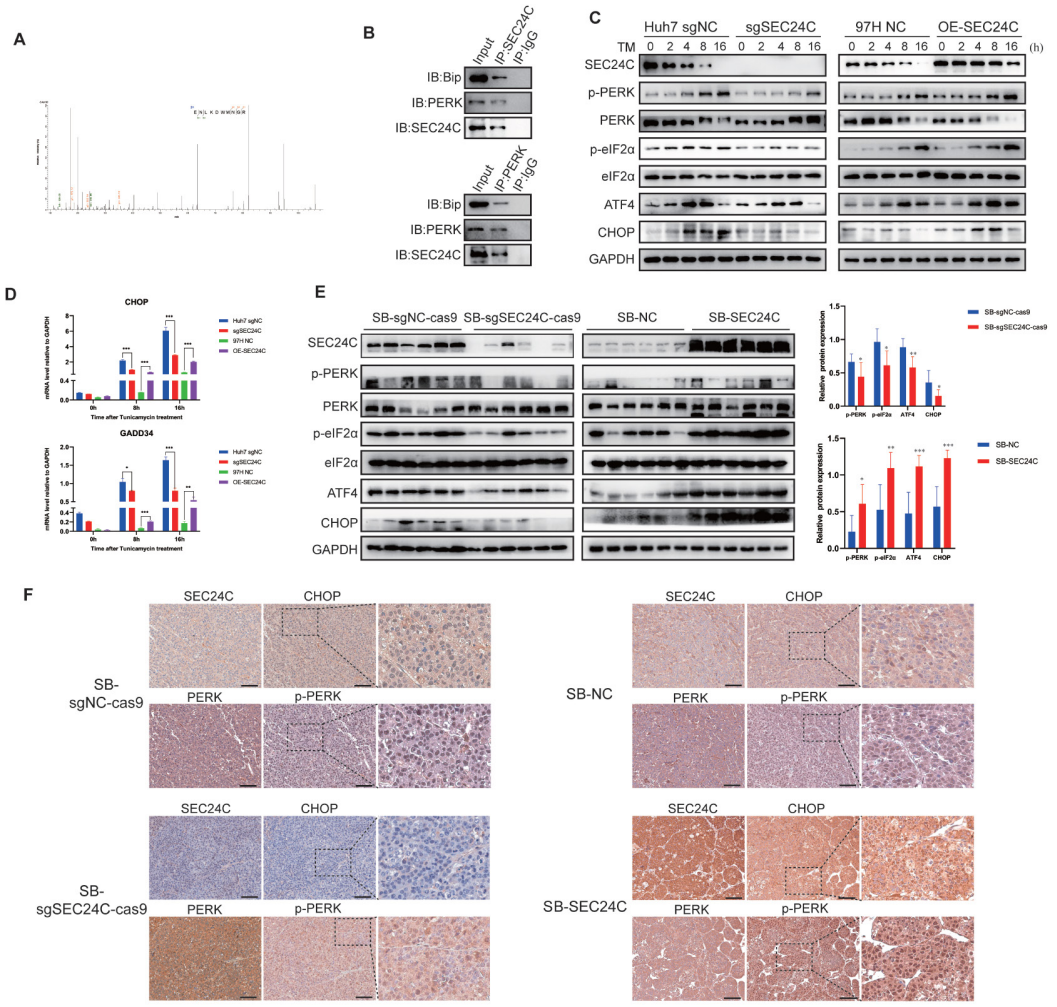

Figure 5. SEC24C modulates activation of the UPR *in vitro* and *in vivo*. (A) A representative PERK tryptic peptide identified in mass spectrometry (MS) analysis of SEC24C-interacting proteins. **(B)** Interaction of the endogenous SEC24C with PERK and Bip determined by Co-IP analysis in Hep3B cells. **(C)** Western blot analysis of the protein levels of phosphorylated PERK, PERK, phosphorylated eIF2α, eIF2α, ATF4 and CHOP after SEC24C knockout or overexpression following tunicamycin treatment. **(D)** qRT–PCR analysis of the mRNA levels of CHOP and GADD34 after SEC24C knockout or overexpression following tunicamycin treatment. (n = 3) **(E)** Western blot analysis of the protein levels of phosphorylated PERK, PERK, phosphorylated eIF2α, eIF2α, ATF4 and CHOP in HCC samples obtained from the $Trp53^{Ahep}$ mice injected with the different plasmids. The quantification of bands is represented in the right bar graph. **(F)** Representative IHC staining images of SEC24C, p-PERK, PERK and CHOP in HCC samples derived from $Trp53^{Ahep}$ mice injected with the different plasmids. Scale bar: 100 μm. All results are presented as the mean ± SD (*P < 0.05; **P < 0.01; ***P < 0.001).

(Supporting Figure S3D, *https://www.biosciencetrends.com/supplementaldata/207*). We also found the significant positive correlations between SEC24C and other UPR target genes (Supporting Figure S3E, *https://www.biosciencetrends.com/supplementaldata/207*). Overall, our data strongly suggested that SEC24C can promote the activation of the PERK-eIF2α-ATF4 branch of the UPR to increase UPR-related apoptosis in HCC.

3.6. SEC24C promotes the UPR by interfering with the interaction between Bip and PERK

To understand the underlying molecular mechanisms by which SEC24C promoted PERK activation in HCC, we sought to explore the potential interaction between Bip, PERK and SEC24C (*4*). First, Co-IP experiments demonstrated the dissociation of Bip away from PERK and SEC24C with BafA1 under ER-stress conditions (Figure 6A, left panel). However, the direct interaction between SEC24C and PERK was increased under ER-stress (Figure 6A, right panel), which suggested that SEC24C could suppress the interaction between Bip and PERK. As expected, SEC24C knockout increased the interaction between Bip and PERK after TM treatment, whereas SEC24C overexpression limited this interaction even under the normal conditions (Figure 6B). Moreover, consistent with the Co-IP results, IF staining demonstrated an interaction between SEC24C and PERK, which was found to be upregulated under ER-stress (Figure 6C). To better understand the roles of precise SEC24C domains that could be essential for this interaction, SEC24C-Flag truncations were constructed and transfected into the Hep3B cells. Co-IP results revealed that residues 748–843 of SEC24C

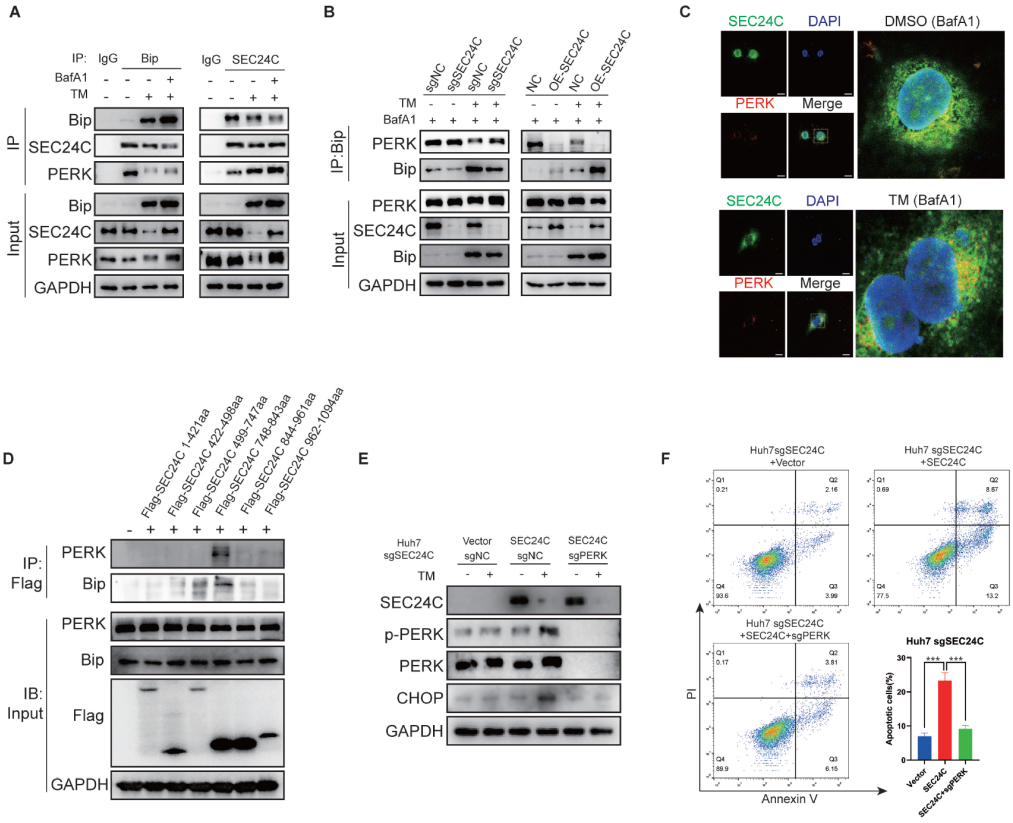

Figure 6. SEC24C interacts with PERK and facilitates the disassociation of Bip from PERK. (A) Immunoprecipitation was performed in Hep3B cells to analyze the protein levels of PERK interacting with Bip (left panel) or SEC24C (right panel) after tunicamycin treatment. **(B)** Immunoprecipitation analysis of PERK and SESC24C proteins interacting with Bip after treatment with DMSO or tunicamycin upon SEC24C variation in the corresponding Huh7 or MHCC97H cells. **(C)** Representative immunofluorescence staining images displaying the colocalization of SEC24C and PERK in HCC cells treated with DMSO or TM in Huh7 cells (scale bar: 25 μm). **(D)** Hep3B cells were transfected with the different Flag-SEC24C truncations. Immunoprecipitations were performed with anti-Flag antibodies to identify the individual binding sites of SEC24C. **(E)** Huh7 sgSEC24C cells were transfected with the various indicated plasmids, such as vector, SEC24C, sgNC or sgPERK-cas9, and treated with DMSO or TM to examine the CHOP expression upon variation of SEC24C and PERK. **(F)** Apoptosis assays for Huh7 sgSEC24 cells transfected with indicated plasmids were performed after the treatment with DMSO or TM for 36 hours using flow cytometry analysis. The apoptosis rate of the cells was measured and has been shown in right lower bar graph. All experiments were performed in triplicate, and the data has been expressed as the mean ± SD from three independent experiments ($n = 3$, $^{***}P < 0.001$). Abbreviations: DAPI, 4′,6-diamidino-2-phenylindole; IgG, immunoglobulin.

were indispensable for binding to PERK (Figure 6D). Furthermore, we noted that re-expressing SEC24C in Huh7 sgSEC24C cells restored the restrained protein levels of p-PERK and CHOP, which was subsequently inhibited upon PERK knockout (Figure 6E). The results of apoptosis assays also showed that re-expressing SEC24C in SEC24C knockout cells attenuated the anti-apoptotic effect under ER-stress, which was reversed by PERK knockout (Figure 6F).

To further investigate whether loss of SEC24C promotes HCC progression through affecting the PERK-eIF2α-ATF4 pathway, we used various pharmacological modulators targeting the UPR. The results indicated that administration of Sal003, an inhibitor targeting eIF2α phosphatases to prevent the dephosphorylation of eIF2α (*29*), was able to cause upregulated expression of CHOP independent of SEC24C level and significantly suppress upregulated proliferation ability of Huh7 sgSEC24C cells (Supporting Figure S4A-C, *https://www.biosciencetrends.com/supplementaldata/207*). Besides, ISRIB, a potent inhibitor of PERK signaling, significantly rescued the downregulated proliferation ability of MHCC97H OE-SEC24C cells, which also caused a reduction in endogenous production of CHOP (Supporting Figure S4D-S4F, *https://www.biosciencetrends.com/supplementaldata/207*). Thus, our findings indicated that SEC24C increased the dissociation of Bip from PERK and activated downstream CHOP-related apoptosis, which in turn could attenuate the malignant phenotypes of HCC cells.

3.7. SEC24C increases the chemosensitivity of HCC to Bortezomib

In recent years, induction of lethal ER-stress or suppression of the cytoprotective UPR has emerged as a new target for cancer therapy (*2,4*).As bortezomib (BTZ) was reported to fulfil its anti-tumor function partly through activating UPR and the effect could be strongly inhibited by suppression of ATF4 (*30*), we wondered whether SEC24C could influence the chemosensitivity of HCC to BTZ through regulating

UPR activation. As expected, BTZ obviously upregulated the activation of the PERK-eIF2α-ATF4 axis, and knockdown of SEC24C significantly downregulated but SEC24C overexpression increased the CHOP level in HCC cells treated with BTZ (Figure 7A). Results showed that BTZ significantly inhibited the colony formation and metastatic ability of HCC cells, especially in SEC24C-overexpressing group (Figure 7B). And in SEC24C knockout Huh7 cells, the half-maximal inhibitory concentration (IC_{50}) of BTZ was increased from 12.88 to 19.94 compared with control cells. In SEC24C overexpressing 97H cells, the IC50 of BTZ was decreased from 11.7 to 8.284 compared with control cells (Figure 7C). Next, experiment conducted in xenograft tumor model revealed that SEC24C rendered HCC tumors more sensitive to BTZ toxicity (Figure 7D, 7E). And histological analysis revealed a significantly greater extent of necrosis in the SEC24C-overexpressing group upon BTZ treatment in comparison to any other group (Figure 7F). Sal003 was also administered to immunodeficient xenograft mice with Huh7 sgNC or Huh7 sgSEC24C tumors, and results indicated that both Huh7 sgSEC24C and Huh7 sgNC tumors showed similar sensitivity to Sal003 (Supporting Figure S5, *https://www.biosciencetrends.com/supplementaldata/207*). Overall, these findings indicated that SEC24C overexpression markedly enhanced the chemosensitivity of HCC cells to BTZ induced UPR.

4. Discussion

SEC24C, a member of the Sec24 subfamily of the Sec23/Sec24 family, is an important member of the coat protein complex—COPII. However, to date, little research has been performed to understand the functions of SEC24C in cancer, especially in HCC. In the present study, we have found that SEC24C protein levels were frequently downregulated in HCC tissues in comparison to the peritumor and normal

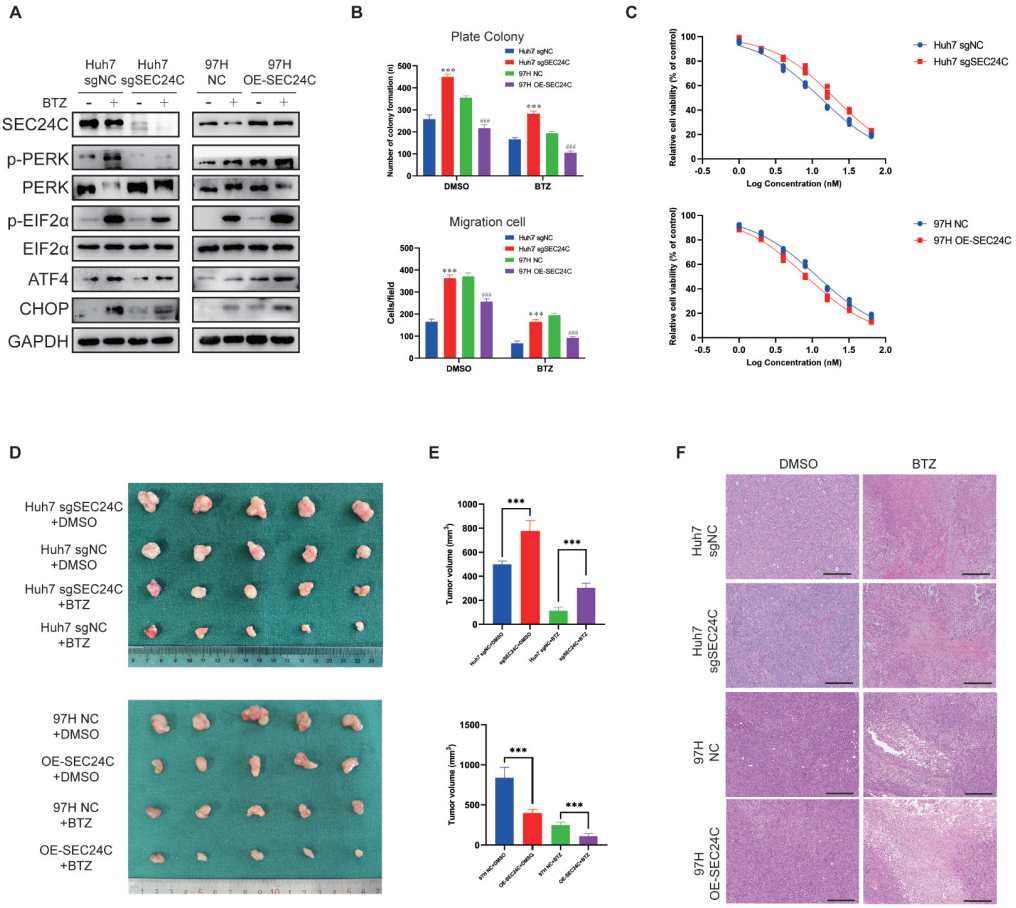

Figure 7. SEC24C promotes the chemosensitivity of HCC to bortezomib. (A) Analysis of protein levels of the PERK-eIF2α-ATF4 axis and CHOP with bortezomib in Huh7 sgSEC24C, MHCC97H OE-SEC24C and their respective control cells. **(B)** The colony formation and migration assays are induced by Huh7 sgSEC24C, MHCC97H OE-SEC24C and their control cells with DMSO or BTZ. The number of colonies and migrated cells were measured and shown in the bar graph ($n = 3$). **(C)** The cell viability was measured with CCK8 assay in Huh7 sgSEC24C, MHCC97H OE-SEC24C and their control cells with the indicated concentrations of BTZ. **(D)** Representative images are shown for the tumors derived from nude mice induced by Huh7 sgSEC24C and Huh7 sgNC cells (upper panel) and MHCC97H OE-SEC24C and MHCC97H NC cells (lower panel) with tail vein injection of vehicle or bortezomib. The tumor weight and volume of each group of mice have been summarized in right panels **(E)** ($n = 5$). **(F)** Xenografts were fixed and embedded in the paraffin and stained with hematoxylin and eosin for analysis of tumor necrosis induced by BTZ. All the data has been expressed as the mean ± SD from three independent experiments. Scale bars = 250 μm. (*$P < 0.05$; **$P < 0.01$; ***$P < 0.001$).

liver tissues. In addition, SEC24C levels were found to be negatively correlated with poor prognosis in HCC patients. Thereafter, through a series of *in vitro* as well as *in vivo* experiments, the potential role of SEC24C in regulating HCC cell proliferation, migration, invasion and apoptosis resistance was examined.

The basic UPR pathway is primarily divided into three branches initiated by three distinct ER transmembrane protein sensors: PERK, inositol-requiring enzyme 1α and activating transcription factor 6 (*31*). Under conditions of ER homeostasis, Bip bind to these sensors and prevent their activation. But upon ER-stress, BiP display higher affinity for various misfolded proteins and dissociate from these sensors (*32*). Thereafter PERK can phosphorylate itself and leads to the activation of eIF2α, which in turn can reduce global protein synthesis and suppresses proliferation, while selectively increasing ATF4 expression. Prolonged or extreme ER-stress lead to the subsequent transcriptional upregulation of CHOP and GADD34. As a transcription factor, CHOP can translocate to the nucleus and can facilitate programmed cell death by upregulating various genes involved in apoptosis (*33*). The loss of CHOP can render the cells and mice more resistant to ER-stress (*34*). In summary, moderate ER-stress responses caused by conditions of the tumor microenvironment promote cancer cell proliferation, metastasis and chemoresistance, but extreme ER-stress lead to a terminal UPR to induce cell death (*4*).

Our data clearly showed that SEC24C could localize in the nucleus with NPM1 under normal condition but respond rapidly to ER-stress and subsequently translocate at the ER surface. In previous report, NPM1 could shuttle to cytoplasm under stressed conditions, and our study also found its reduction upon ER-stress. As SEC24C has no classic nuclear localization signal, the localization of SEC24C in nucleus may rely on the interaction with NPM1, which could regulate nuclear import of protein without nuclear localization signal (*20*). When ER-stress are continuously activated, the expression of NPM1 in nucleus would be decreased, then SEC24C in the nucleus would shuttle to the ER surface for replenishing its deficiency by autolysosome degradation. The mechanism of NPM1 reduction upon ER-stress and the function of SEC24C in nucleus need our future exploration. In addition, we also found that SEC24C overexpression provoke extreme activation of the PERK-eIF2α-ATF4 axis and redirect the cells to CHOP-related apoptotic death. Thus, the shuttling ability of SEC24C between nucleus and ER are significant for the rapid response of hepatocytes to ER-stress and help prevent massive localization of SEC24C on ER for UPR activation under normal conditions. So, the hyperactive ER-phagy in HCC may partially account for the deficiency of SEC24C and subsequently enable HCC cells to tolerate to extreme ER-stress and escape from final UPR-related apoptosis.

BTZ, an FDA-approved drug, has been reported to markedly decrease the viability of HCC cells partly through UPR and the effect could be strongly inhibited by suppression of ATF4 (*30*). We found that overexpression of SEC24C significantly promote the sensitivity of HCC cells to BTZ treatment under both *in vitro* and *in vivo* settings. In addition, prior studies have also reported that the eIF2α-specific phosphatase inhibitor salubrinal inhibit the progression of HCC cells and its derivative Sal003 could also inhibit breast cancer progression (*30,35*). Our results demonstrated that the tumor volume of the nude mice with Huh7 sgNC and Huh7 sgSEC24C was reduced to a similar volume after the treatment with Sal003, thus suggesting that targeting downstream eIF2α could be a promising strategy to treat HCC tumors with low SEC24C expression.

In summary, our findings revealed that SEC24C can significantly suppress both HCC propagation and chemoresistance by promoting activation of the PERK-CHOP related apoptotic death, which could also partly explain the underlined mechanism of HCC cells escaping from apoptosis and maintaining proliferation under persistent ER-stress *via* SEC24C deficiency. Besides, by employing BTZ and several modulators targeting UPR signaling pathway, this present study can also provide opportunities for selecting appropriate chemotherapeutic drugs according to SEC24C expression levels in HCC tumors.

Acknowledgements

We would like to thank all laboratory members for their critical discussion of this manuscript.

Funding: This work was supported by grants from National Natural Science Foundation of China (82101850) & Project funded by China Postdoctoral Science Foundation (2021M701679) To Y.L.

Conflict of Interest: The authors have no conflicts of interest to disclose.

Ethics Approval and Consent to Participate: HCC samples (including tumor and adjacent nontumor samples) were collected from patients between August 2019 and September 2022 at Nanjing Drum Tower Hospital. Normal human liver samples were obtained from hepatic hemangioma patients with no evidence of chronic liver disease, diabetes, or hypertension. All patients provided written consent. All studies were approved by the Institutional Ethics Committee of Nanjing Drum Tower Hospital in compliance with the 1975 Declaration of Helsinki.

Availability of Data and Materials: The data generated in this study are available within the article and its

supplementary data files. Extra expression profile data analyzed in this study were obtained from TGCA dataset for tumor and GTEx dataset for normal. Prognosis data of patients with HCC were obtained from Kaplan-Meier Plotter database (*http://kmplot.com/analysis/index.php?p=service&cancer=liver_rnaseq*).

References

1. Vogel A, Meyer T, Sapisochin G, Salem R, Saborowski A. Hepatocellular carcinoma. Lancet. 2022; 400:1345-1362.
2. Li Z, Ge Y, Dong J, Wang H, Zhao T, Wang X, Liu J, Gao S, Shi L, Yang S, Huang C, Hao J. BZW1 Facilitates Glycolysis and Promotes Tumor Growth in Pancreatic Ductal Adenocarcinoma Through Potentiating eIF2alpha Phosphorylation. Gastroenterology. 2022; 162:1256-1271. e1214.
3. Hetz C, Chevet E, Harding HP. Targeting the unfolded protein response in disease. Nat Rev Drug Discov. 2013; 12:703-719.
4. Chen X, Cubillos-Ruiz JR. Endoplasmic reticulum stress signals in the tumour and its microenvironment. Nat Rev Cancer. 2021; 21:71-88.
5. Hetz C, Zhang K, Kaufman RJ. Mechanisms, regulation and functions of the unfolded protein response. Nat Rev Mol Cell Biol. 2020; 21:421-438.
6. Walter P, Ron D. The unfolded protein response: from stress pathway to homeostatic regulation. Science. 2011; 334:1081-1086.
7. Bernales S, McDonald KL, Walter P. Autophagy counterbalances endoplasmic reticulum expansion during the unfolded protein response. PLoS Biol. 2006; 4:e423.
8. Cui Y, Parashar S, Zahoor M, Needham PG, Mari M, Zhu M, Chen S, Ho HC, Reggiori F, Farhan H, Brodsky JL, Ferro-Novick S. A COPII subunit acts with an autophagy receptor to target endoplasmic reticulum for degradation. Science. 2019; 365:53-60.
9. Zielke S, Kardo S, Zein L, Mari M, Covarrubias-Pinto A, Kinzler MN, Meyer N, Stolz A, Fulda S, Reggiori F, Kogel D, van Wijk S. ATF4 links ER stress with reticulophagy in glioblastoma cells. Autophagy. 2021; 17:2432-2448.
10. Quesada-Calvo F, Massot C, Bertrand V, *et al*. OLFM4, KNG1 and Sec24C identified by proteomics and immunohistochemistry as potential markers of early colorectal cancer stages. Clin Proteomics. 2017; 14:9.
11. Xin C, Diego F CJAJP. Hydrodynamic transfection for generation of novel mouse models for liver cancer research. 2014; 184.
12. Gao Q, Zhu H, Dong L, *et al*. Integrated Proteogenomic Characterization of HBV-Related Hepatocellular Carcinoma. Cell. 2019; 179:1240.
13. Ferro-Novick S, Reggiori F, Brodsky JL. ER-Phagy, ER Homeostasis, and ER Quality Control: Implications for Disease. Trends Biochem Sci. 2021; 46:630-639.
14. Wilkinson S. ER-phagy: shaping up and destressing the endoplasmic reticulum. FEBS J. 2019; 286:2645-2663.
15. Chen Q, Xiao Y, Chai P, Zheng P, Teng J, Chen J. ATL3 Is a Tubular ER-Phagy Receptor for GABARAP-Mediated Selective Autophagy. Curr Biol. 2019; 29:846-855 e846.
16. Klionsky DJ, Abdel-Aziz AK, Abdelfatah S, *et al*. Guidelines for the use and interpretation of assays for monitoring autophagy (4th edition). Autophagy. 2021; 17:1-382.
17. Chino H, Hatta T, Natsume T, Mizushima NJMc. Intrinsically Disordered Protein TEX264 Mediates ER-phagy. 2019; 74:909-921.e906.
18. Grisendi S, Mecucci C, Falini B, Pandolfi PP. Nucleophosmin and cancer. Nat Rev Cancer. 2006; 6:493-505.
19. Borer RA, Lehner CF, Eppenberger HM, Nigg EA. Major nucleolar proteins shuttle between nucleus and cytoplasm. Cell. 1989; 56:379-390.
20. Gao H, Jin S, Song Y, Fu M, Wang M, Liu Z, Wu M, Zhan Q. B23 regulates GADD45a nuclear translocation and contributes to GADD45a-induced cell cycle G2-M arrest. J Biol Chem. 2005; 280:10988-10996.
21. Clarke HJ, Chambers JE, Liniker E, Marciniak SJ. Endoplasmic reticulum stress in malignancy. Cancer Cell. 2014; 25:563-573.
22. Hong F, Lin CY, Yan J, Dong Y, Ouyang Y, Kim D, Zhang X, Liu B, Sun S, Gu W, Li Z. Canopy Homolog 2 contributes to liver oncogenesis by promoting unfolded protein response-dependent destabilization of tumor protein P53. Hepatology. 2022; 76:1587-1601.
23. Tang J, Guo YS, Zhang Y, Yu XL, Li L, Huang W, Li Y, Chen B, Jiang JL, Chen ZN. CD147 induces UPR to inhibit apoptosis and chemosensitivity by increasing the transcription of Bip in hepatocellular carcinoma. Cell Death Differ. 2012; 19:1779-1790.
24. Parashar S, Chidambaram R, Chen S, Liem CR, Griffis E, Lambert GG, Shaner NC, Wortham M, Hay JC, Ferro-Novick S. Endoplasmic reticulum tubules limit the size of misfolded protein condensates. Elife. 2021; 10.
25. Adolf F, Rhiel M, Reckmann I, Wieland FT. Sec24C/D-isoform-specific sorting of the preassembled ER-Golgi Q-SNARE complex. Mol Biol Cell. 2016; 27:2697-2707.
26. Liu Z, Lv Y, Zhao N, Guan G, Wang J. Protein kinase R-like ER kinase and its role in endoplasmic reticulum stress-decided cell fate. Cell Death Dis. 2015; 6:e1822.
27. Marciniak SJ, Yun CY, Oyadomari S, Novoa I, Zhang Y, Jungreis R, Nagata K, Harding HP, Ron D. CHOP induces death by promoting protein synthesis and oxidation in the stressed endoplasmic reticulum. Genes Dev. 2004; 18:3066-3077.
28. Wendeler MW, Paccaud JP, Hauri HP. Role of Sec24 isoforms in selective export of membrane proteins from the endoplasmic reticulum. EMBO Rep. 2007; 8:258-264.
29. Yahiro K, Tsutsuki H, Ogura K, Nagasawa S, Moss J, Noda M. Regulation of subtilase cytotoxin-induced cell death by an RNA-dependent protein kinase-like endoplasmic reticulum kinase-dependent proteasome pathway in HeLa cells. Infect Immun. 2012; 80:1803-1814.
30. Ord T, Ord D, Kaikkonen MU, Ord T. Pharmacological or TRIB3-Mediated Suppression of ATF4 Transcriptional Activity Promotes Hepatoma Cell Resistance to Proteasome Inhibitor Bortezomib. Cancers (Basel). 2021; 13.
31. Ron D, Walter P. Signal integration in the endoplasmic reticulum unfolded protein response. Nat Rev Mol Cell Biol. 2007; 8:519-529.
32. Wang M, Wey S, Zhang Y, Ye R, Lee AS. Role of the unfolded protein response regulator GRP78/BiP in development, cancer, and neurological disorders. Antioxid Redox Signal. 2009; 11:2307-2316.
33. Samanta S, Yang S, Debnath B, Xue D, Kuang Y, Ramkumar K, Lee AS, Ljungman M, Neamati N. The Hydroxyquinoline Analogue YUM70 Inhibits GRP78

to Induce ER Stress-Mediated Apoptosis in Pancreatic Cancer. Cancer Res. 2021; 81:1883-1895.
34. Han J, Back SH, Hur J, Lin YH, Gildersleeve R, Shan J, Yuan CL, Krokowski D, Wang S, Hatzoglou M, Kilberg MS, Sartor MA, Kaufman RJ. ER-stress-induced transcriptional regulation increases protein synthesis leading to cell death. Nat Cell Biol. 2013; 15:481-490.
35. Darini C, Ghaddar N, Chabot C, *et al*. An integrated stress response *via* PKR suppresses HER2+ cancers and improves trastuzumab therapy. Nat Commun. 2019; 10:2139.

Received June 4, 2024; Revised July 10, 2024; Accepted July 23, 2024.

[§]These authors contributed equally to this work.

*Address correspondence to:
Beicheng Sun, School of Medicine, Southeast University, Nanjing 210009, Jiangsu, China.
E-mail: sunbc@nju.edu.cn

Yang Liu, Department of General Surgery, The First Affiliated Hospital of Anhui Medical University, Hefei 230022, Anhui, China.
E-mail: liuyang_1005@163.com

Jincheng Wang, Graduate School of Medical Science and Engineering, Hokkaido University, Sapporo, Japan.
E-mail: jcwang_med@hotmail.com

Released online in J-STAGE as advance publication August 1, 2024.